

# Exploring Scalability of Self-Training for Open-Vocabulary Temporal Action Localization

Jeongseok Hyun<sup>1</sup>   Su Ho Han<sup>1</sup>   Hyolim Kang<sup>1</sup>  
Joon-Young Lee<sup>2</sup>   Seon Joo Kim<sup>1</sup>

<sup>1</sup>Yonsei University   <sup>2</sup>Adobe Research

**Abstract.** The vocabulary size in temporal action localization (TAL) is constrained by the scarcity of large-scale annotated datasets. To address this, recent works incorporate powerful pre-trained vision-language models (VLMs), such as CLIP, to perform open-vocabulary TAL (OV-TAL). However, unlike VLMs trained on extensive image/video-text pairs, existing OV-TAL methods still rely on small, fully labeled TAL datasets for training an action localizer. In this paper, we explore the scalability of self-training with unlabeled YouTube videos for OV-TAL. Our self-training approach consists of two stages. First, a class-agnostic action localizer is trained on a human-labeled TAL dataset and used to generate pseudo-labels for unlabeled videos. Second, the large-scale pseudo-labeled dataset is combined with the human-labeled dataset to train the localizer. Extensive experiments demonstrate that leveraging web-scale videos in self-training significantly enhances the generalizability of an action localizer. Additionally, we highlighted issues with existing OV-TAL evaluation schemes and proposed a new evaluation protocol. Code is released at <https://github.com/HYUNJS/STOV-TAL>.

**Keywords:** Open-Vocabulary learning · Temporal action localization · Self-Training

## 1 Introduction

Temporal action localization (TAL) involves localizing and classifying action instances in long videos. However, annotating large TAL datasets with extensive action vocabularies is costly, limiting models to small vocabularies. Developing TAL models that cover any target actions has been a long-standing goal.

As relevant research directions, Open-set TAL [1] aims to localize all actions by assigning base classes and marking novel actions as unknown, and Open-world TAL [50] extends open-set TAL by integrating continual learning, where the model is updated with annotations of novel actions after the initial training phase. However, both settings are not suitable to achieve the goal since they cannot classify unseen actions. In contrast, recent works [29, 49] adopted a zero-shot (ZS) learning approach, leveraging semantic information from language models [10, 27] to classify unseen actions. However, as the main goal in ZS learning is to recognize concepts not seen during training [42], it strictly restricts the use of samples of unseen action classes for training. This stringent restriction hinders scaling TAL models with large-scale web data.

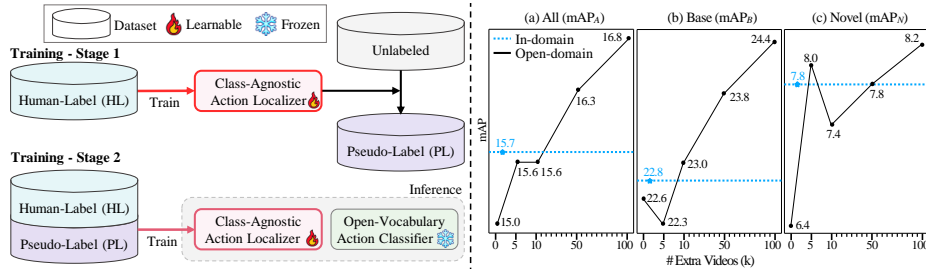


**Fig. 1: (Left)** Our two-stage pipeline starts by training a class-agnostic action localizer on a human-labeled (HL) TAL dataset. Then, it generates pseudo-labels (PL) for unlabeled videos. Due to high annotation costs, HL is limited in volume and category, whereas PL is free from them. The combined dataset is then used to train the localizer, enhancing its generalization across diverse action categories and video domains. **(Right)** Two types of data sources are explored: in-domain, including videos from novel categories of the target benchmark, and open-domain, including random web videos. The scalability of our self-training approach is demonstrated by increasing mAPs.

Different from ZS learning, Zareian *et al.* [47] proposed open-vocabulary (OV) learning for object detection that alleviates the restriction of training data. Specifically, OV learning leverages image-text pairs for training, where the classes used for testing may or may not be present in the training data. This relaxed constraint allows vision-language models (VLMs) like CLIP [33], which are pre-trained on extensive image-caption pairs, to demonstrate robust zero-shot performance across various tasks, including open vocabulary temporal action localization (OV-TAL).

Existing OV-TAL methods [15, 28, 32] utilize a VLM for classification. Nevertheless, their class-agnostic action localizers continue to rely on small, fully labeled TAL datasets, even within the OV learning framework. This approach overlooks the vast potential of numerous web videos for enhancing action localization. To address this, we explore self-training with additional unlabeled videos to improve the **generalization capability of action localization**. Although the class-agnostic action localizer can already detect the novel actions [20], we found that self-training with large-scale web video can improve cross-category generalization capabilities. Our training pipeline is illustrated in Fig. 1 (Left).

We study two types of data sources for self-training: in-domain and open-domain. In-domain data is acquired by splitting the target benchmark, indicating that it includes videos from novel categories of the target benchmark. On the other hand, Open-domain data includes random web videos. Although in-domain data is considered gold data, it is confined to the benchmark. In contrast, open-domain data is a scalable source as more videos can be scraped from the web. Fig. 1 (Right) shows the results on the FineAction dataset [23], which covers various video domains. Using 100k random videos, we surpass the performance of in-domain data for both base and novel classes. This proves the effectiveness of self-training with web videos. More scaling results are presented in Tab. 1.

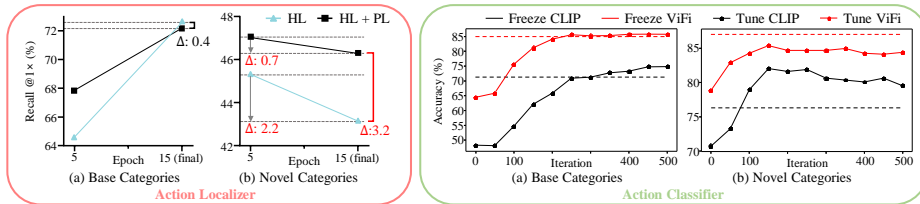


**Fig. 2:** Changes in model generalization ability when training on a human-labeled (HL) dataset of base categories. **(Left)** Training an action localizer on HL significantly reduces performance on novel categories; this issue is mitigated through our self-training approach. **(Right)** Partial tuning of VLM (CLIP [33]) initially increases accuracy for novel categories but leads to decreased accuracy as base category accuracy saturates. In contrast, ViFi-CLIP [34], fully tuned on a large video dataset, achieves higher accuracy. However, partially tuning ViFi-CLIP on a small-scale TAL dataset (thumos14 [13]) diminishes its novel category accuracy, indicating a loss of generalization ability.

We also explore changes in generalization ability when the action localizer and classifier are trained on a human-labeled TAL dataset of base categories. Following EffPrompt [15], we partially tune a VLM by adding a transformer layer on the visual encoder and learnable prompts on the text encoder. Fig. 2 shows that the performance of both localizer and classifier decreases in novel actions while base actions performance saturates. When the action localizer is trained with our self-training approach, such loss of generalization ability can be prevented. ViFi-CLIP, which is already fine-tuned on large video-text data, does not benefit from partial tuning on a TAL dataset and is instead negatively affected by it.

Furthermore, the results indicate that the model with optimal performance in novel actions is under-fitted to base actions. In other words, a meticulous training strategy [26, 52] is required to prevent overfitting to base actions. However, existing evaluation schemes do not assess base actions but only novel actions that are randomly sampled, leading to potentially misleading interpretations. For the proper evaluation, we propose new OV-TAL benchmarks with two features. First, we introduce the generalized zero-shot setting, where the target categories are the union of base and novel, and report the accuracy of all, base, and novel actions, respectively. Base and novel actions are divided using Kinetics dataset [7]. Second, we introduce cross-dataset evaluation that rigorously tests the generalization capability for OV-TAL across domains.

Our contributions can be summarized as follows:

- We show the effectiveness and scalability of exploiting unlabeled videos with self-training to acquire cross-category generalization ability for OV-TAL.
- We introduce new benchmarks for rigorous evaluation of OV-TAL: generalized zero-shot setting with Kinetics based category split and cross-dataset generalization.

## 2 Related Works

### 2.1 Beyond Closed-Vocabulary TAL

**Pre-VLM Era.** Enlarging the vocabulary size of TAL models has been a long-standing goal, studied even before the advent of VLMs. AherNet [24] exploits the combination of TAL and action classification datasets to expand the vocabulary size of TAL through adversarial learning, but its vocabulary size is still limited to the training dataset. Aiming to generalize to unseen actions, Zhang *et al.* [49] explored zero-shot learning in TAL by leveraging the language model embeddings [27] of seen and unseen actions. OpenTAL [1] tackles the open-set setting that localizes and classifies unseen actions as the unknown category on top of seen actions based on the learned evidential uncertainty.

**Post-VLM Era.** Recently, OV-TAL has been explored based on a VLM [33]. The decoupled framework consists of a class-agnostic action localizer and an open-vocabulary action classifier is studied in [15, 16, 35]. Ju *et al.* [15] adapted CLIP [33] for the video domain with extra learnable modules: learnable prompts and transformer encoder for temporal modeling. In the follow-up [16], the prompt tuning method is further studied, such as LLM-generated and visually conditioned prompting, and the use of optical flow with VLM is introduced. Rathod *et al.* [35] explored the performance using different VLMs [14, 31, 33] and modalities including optical flow and audio. STALE [28] is the one-stage framework while UnLoc [46] unifies other video localization tasks, such as action segmentation and moment retrieval.

**Our Work.** We explore the scalability of self-training with web videos for OV-TAL, especially aiming to enhance the generalization ability of “action localization”.

### 2.2 Vision-Language Models

**Image VLMs.** CLIP [33] shows remarkable performance in zero-shot image recognition, and the generalization ability is demonstrated across diverse domains. This is attributed to the utilization of large-scale image-text datasets scraped from the web. For example, CLIP [33] and OpenCLIP [8] are trained on 400M and 2B image-text pairs. Such scalability offers benefits over manually annotated datasets, such as ImageNet-21k [9] with 14M images.

**Video VLMs.** Compared to image VLMs, video VLMs are under-explored due to a lack of large-scale video-caption datasets. Initially, image VLMs are adapted to the video domain with prompt tuning and extra transformer layers to capture the temporal relationship [15, 30]. ViFi-CLIP [34] shows that simply fine-tuning CLIP in video snippets without temporal modeling improves the performance. Open-VCLIP [41] prevents the loss of generalization during video fine-tuning of CLIP through the regularization method. MAXI [22] explores the use of LLMs [4, 18] to generate video-caption pairs in the Kinetics videos [7] while ViCLIP [39] is trained on InternVid [39] dataset composed of 234M pairs.

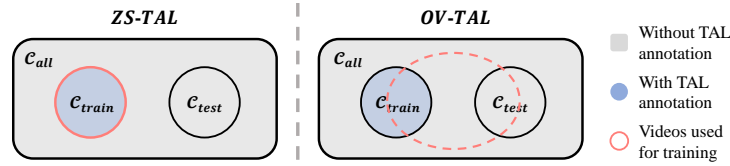


**Fig. 3: Comparison of ZS-TAL and OV-TAL training.** In ZS-TAL, a training dataset is confined to  $\mathcal{C}_{train}$  which is strictly separated from  $\mathcal{C}_{test}$ . OV-TAL allows the use of videos without TAL labels even if the videos may contain actions of  $\mathcal{C}_{test}$ .

**Our Work.** We adopt ViFi-CLIP [34] as the frozen VLM in the proposed framework while the recently proposed ones can also be adopted.

### 3 Methodology

To encompass largely available unlabeled untrimmed video to TAL, we adopt the open-vocabulary learning setting into TAL. As a solution, we propose the framework, **Self-Training for Open-Vocabulary Temporal Action Localization**, namely, **STOV-TAL**. This section provides a rigorous definition of this setting with the evaluation protocol. Then, we describe the straightforward yet effective architecture and the training method that improves the generalization ability of action localization.

#### 3.1 Problem Definition of OV-TAL

Input for OV-TAL consists of an untrimmed video,  $\mathcal{V}$ , and  $C$  number of target action categories,  $\mathcal{C} = \{c_i\}_{i=1}^C$ , which are unbounded and can be flexibly manipulated by users. Its output consists of  $M$  action instances,  $\Psi = \{(t_s, t_e, c, s)_i\}_{i=1}^M$ , where  $t_s$ ,  $t_e$ ,  $c$ , and  $s$  denote the start and end times of the action, the action category, and the confidence score, respectively.

Regarding the training data utilization, the OV-TAL setting offers a more flexible approach, as depicted in Fig. 3. In ZS-TAL, training data is limited to videos with human-annotated TAL labels corresponding to  $\mathcal{C}_{train}$  which is a disjoint set following  $\mathcal{C}_{train} \cap \mathcal{C}_{test} = \emptyset$ . However, the OV-TAL setting relaxes this strict restriction of training data. Specifically, we do not limit the use of data sources which may include actions of  $\mathcal{C}_{test}$  unless the TAL annotations are provided together. This allows for the incorporation of abundant unlabeled, random videos from the web. As a result, training the action localizer is no longer limited to the small-scale TAL datasets; instead, it involves exploiting data with diverse categories and domains. Therefore, the OV-TAL setting is more suitable for exploring generalization ability.

#### 3.2 Evaluation Protocol for OV-TAL

Existing ZS-TAL benchmarks [15] face two issues: (1) they do not evaluate the seen categories, but only unseen categories, and (2) they rely on random category splits that do not consider the category frequency. To address these, we introduce

the generalized ZS evaluation setting with the Kinetics-based [7] category split on the proposed OV-TAL benchmarks. The proposed benchmarks are crucial at this stage for advancing OV-TAL further.

**Generalized Zero-Shot Evaluation.** As shown by Fig. 3, the benchmark dataset is disjointly divided. In the ZS-TAL benchmark, the model is trained on the training videos of  $\mathcal{C}_{train}$  and is evaluated on the validation videos of  $\mathcal{C}_{test}$ , *i.e.*,  $\mathcal{C}_{target} = \mathcal{C}_{test}$ . In this way, setting the target categories by either  $\mathcal{C}_{train}$  or  $\mathcal{C}_{test}$  is referred to the constrained zero-shot evaluation protocol. As pointed out by Xian *et al.* [44], the constrained setting provides strong prior knowledge and makes the problem easier by not considering  $\mathcal{C}_{train}$ , which are used for optimizing the model. On the contrary, the generalized zero-shot evaluation protocol includes all categories in the benchmark for evaluation, *i.e.*,  $\mathcal{C}_{target} = \mathcal{C}_{train} \cup \mathcal{C}_{test}$ . In addition to the accuracy of all categories, we also measure the accuracy of  $\mathcal{C}_{train}$  and  $\mathcal{C}_{test}$  under this generalized protocol.

**Category Split.** Existing ZS-TAL benchmarks are based on the splits whose categories are randomly chosen [15, 49]. Ju *et al.* [15] proposed ten random splits with ratios, *e.g.*, 50%–50% for  $\mathcal{C}_{train}$  and  $\mathcal{C}_{test}$ , and the final accuracy is computed by averaging the results of each split. In our Kinetics-based split, we regard actions covered in Kinetics as common categories and use them as base categories ( $\mathcal{C}_B$ ); those not covered are considered rare actions and treated as novel categories ( $\mathcal{C}_N$ ). Two reasons support this criterion: (1) The action list in K400 is thoughtfully selected to encompass actions that are commonly encountered in daily life. This selection criterion allows us to simulate a challenging scenario where categories of varying frequency - frequent for training and infrequent for testing - are utilized. (2) K400 is a common choice for pre-training video backbones, and detecting actions not present in K400 can demonstrate a more rigorous test of category generalization ability.

To automatically detect the category overlap, we utilize NLTK [2] to perform stemming and lemmatization on the text of action categories and verify whether the words of action category in the benchmark are present in the set of K400 actions. After this process, we derive the sets of  $(|\mathcal{C}_B|, |\mathcal{C}_N|)$  as (90, 110), (12, 8), and (56, 50) for ActivityNet v1.3, THUMOS14, and FineAction, respectively.

### 3.3 STOV-TAL Architecture

We decouple the localization and classification of actions into two components in the architecture: (1) class-agnostic action localizer; (2) open-vocabulary action classifier based on the video VLM [34]. Fig. 4 illustrates the detailed pipeline. Note that this architecture supports various CLIP-like VLMs, which typically include separate uni-modal encoders for video and text, represented as the video encoder ( $\Phi_V$ ) and the text encoder ( $\Phi_T$ ).

**Video Feature Extraction with VLM.** Frames are sampled from the input video using the overlapping sliding window approach, commonly used in the TAL literature [48]. This takes consecutive frames of window size and slides a window

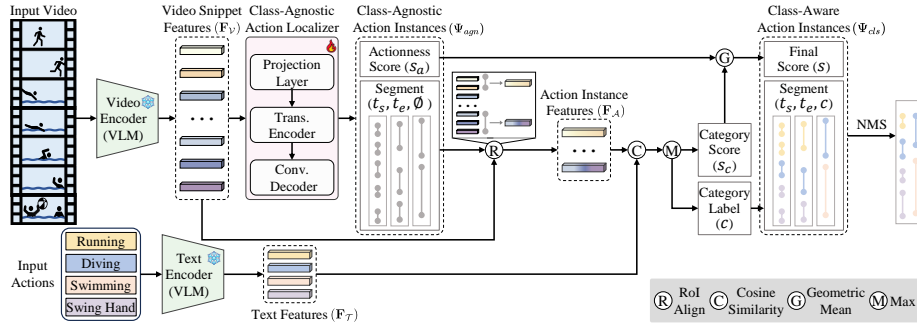


**Fig. 4: Architecture.** Features  $\mathbf{F}_V$  and  $\mathbf{F}_T$  are generated by VLM video and text encoders from video frames and action names, respectively. The action localizer detects class-agnostic action instances, and their features ( $\mathbf{F}_A$ ) are extracted using RoI-Align. Cosine similarities between  $\mathbf{F}_A$  and  $\mathbf{F}_T$  are computed to assign the top-scoring category to each action instance. The category score ( $s_c$ ) is averaged with its actionness score ( $s_a$ ) to obtain the final confidence score ( $s$ ).

with the stride size. As a result, a long untrimmed video is divided into multiple overlapping video snippets, represented as  $\mathcal{V} = \{\mathcal{V}_i\}_{i=1}^S \in \mathbb{R}^{S \times T \times H \times W \times 3}$ , where  $S$  is the number of snippets and  $T$  is the window size. For each snippet, the VLM’s video encoder outputs the feature vector,  $\Phi_V(\mathcal{V}_i) \in \mathbb{R}^D$ , where  $D$  is the dimension of the feature. By processing the entire video, we obtain the video snippet features,  $\mathbf{F}_V = \Phi_V(\mathcal{V}) \in \mathbb{R}^{S \times D}$ .

**Detecting Every Action.** In this stage, the primary goal is to detect every action instance with its actionness score  $s_a$ , rather than predicting its action category. To achieve this goal, we employ the action localizer that produces class-agnostic action instances, represented as  $\Psi_{agn} = \{(t_s, t_e, \emptyset, s_a)_i\}_{i=1}^M$ . Here,  $\emptyset$  indicates the absence of the action category. Our framework offers flexibility in selecting the architecture of the action localizer, provided that the output format is compatible. It accommodates both two-stage methods [20, 45] and one-stage methods [19, 48] when trained in a class-agnostic manner. The class-agnostic action localizer is improved with stronger generalization ability through the proposed self-training process, detailed in Sec. 3.4.

To make the paper self-contained, we provide a concise overview of the adopted action localizer [48]. This localizer includes a convolutional projection layer, a multi-scale transformer encoder, and parallel convolutional decoders in sequence, as described in the action localizer block of Fig. 4. The first two modules update the video snippet features to consider both temporal locality and long-term contexts. Temporal downsampling operations are integrated into the encoder to extract multi-scale features for capturing the actions at different temporal scales due to the varying granularity of actions. Two parallel convolutional decoders are used to predict the actionness score and the offset for start and end time in every snippet across the temporal axis at each scale.

**Classifying Every Action.** We use an open-vocabulary action classifier for assigning the most appropriate action category ( $c$ ) among the input actions to the previously detected action instances ( $\Psi_{agn}$ ), resulting in the class-aware action instances ( $\Psi_{cls}$ ). Following CLIP [33], the input actions are tokenized by the lower-cased byte pair encoding [36] with the start and end tokens. The tokenized actions are encoded through the VLM’s text encoder as the text features,  $\mathbf{F}_{\mathcal{T}} \in \mathbb{R}^{C \times D}$ , where  $C$  is the number of input action categories. The visual features of each action instance are extracted from the VLM’s video snippet features by the RoI-Align operation [12] with its start and end times. Then, we obtain  $\mathbf{F}_{\mathcal{A}} \in \mathbb{R}^{M \times D}$ , where  $M$  is the number of instances.

Based on these features, we compute the cosine similarity between  $\mathbf{F}_{\mathcal{A}}$  and  $\mathbf{F}_{\mathcal{T}}$ , which is a matrix of  $\mathbb{R}^{M \times C}$ . It is normalized by the softmax operation in the axis of the category after scaling it by the temperature parameter. This matrix value indicates each instance’s class confidence scores ( $s_c$ ). While we can choose top- $K$  action categories for each instance, we only choose the top-scoring action category as the default setting. Finally, the actionness score,  $s_a$ , and the category confidence score,  $s_c$ , of each action instance are fused by the geometric mean to compute the final confidence score,  $s$ . The output from this stage is class-aware action instances, represented as  $\Psi_{cls} = \{(t_s, t_e, c, s)_i\}_{i=1}^M$ . As the post-processing, softNMS [3] is applied to remove the duplicates and obtain the final action instances.

### 3.4 Learning to Detect Every Action

A class-agnostic action localizer has demonstrated the ability to localize actions that were not seen during training [15, 20]. Leveraging its cross-category generalization ability, our architecture can detect and classify any input actions without requiring specialized training methods. Nonetheless, its generalization ability remains limited, particularly for unseen domains (*i.e.*, cross-dataset evaluation). This is attributed to the small scale of the TAL datasets that lack diverse action categories or domains. Inspired by the semi-supervised learning commonly employed in data-scarce scenarios, we aim to enhance the action localizer’s generalization ability through the self-training method [17, 43]. As illustrated in Fig. 1, self-training comprises two stages: (1) Training a model on a labeled dataset; and (2) Training the model on an unlabeled dataset, using pseudo-labels generated by the previous model.

**Learning from Labeled Videos.** In the first stage, the action localizer is trained using the human-labeled TAL dataset. Since we employ the class-agnostic action localizer, the classification is about distinguishing the foreground or background of actions in a video. As described in Sec 3.3, the output from the two decoders,  $\Psi_{agn}$ , includes the start and end times of the action and the actionness score. These are trained with the DIOU loss [51] and Focal loss [21], respectively.

**Learning from Unlabeled Videos.** In the second stage, we exploit additional unlabeled videos for training. To obtain pseudo-labels of these videos, the action localizer trained in the first stage is employed to generate the class-agnostic

action instances. Note that the raw output includes many duplicated and noisy instances. We use the NMS [3] operation and the fixed threshold value on the actionness score to remove them. Then, this pseudo-dataset is combined with the first stage’s labeled dataset to form the joint dataset. Our pseudo-label selection process requires finding the proper threshold value. In this regard, the sensitivity analysis of pseudo-labels in Sec 4.4 supports the robustness of this process. Although advanced pseudo-labeling methods, such as adaptive thresholding [40], can be adopted, this paper focuses on **exploring the generalization ability of action localization** using the straightforward self-training method.

The process of selecting videos is crucial for self-training, where we explore two distinct settings: (1) Using **in-domain (ID) data**, and (2) Using **open-domain (OD) data**. In the first setting, we employ the training set of the target benchmark without labels. For instance, videos containing novel actions are chosen for self-training in the cross-category evaluation. However, this video sampling policy is geared towards the evaluation dataset. Utilizing videos from the same dataset ensures in-domain, creating a favorable environment for achieving higher accuracy. Also, the scaling-up effect with a larger volume of data is constrained by a fixed and small number of videos. On the other hand, the second setting utilizes random YouTube videos whose video IDs are sourced from K600 [6]. In contrast to the Kinetics dataset, where videos are trimmed to focus on the specific labeled action category, we use untrimmed videos.

The training objectives used in the first stage are also used in this stage. When the scale of the unlabeled dataset is significantly larger than that of the labeled dataset and their distributions differ, the action localizer may struggle to learn robust knowledge from the labeled dataset. Thus, we adopt the Mean Teacher framework [37] and initialize the teacher model with the action localizer trained in the first stage. In this teacher-student framework, the teacher model is used for inference and is updated with the student model in the manner of exponential moving average as formulated in Eq. 1:

$$\theta'_{iter} = (1 - \lambda)\theta_{iter} + \lambda\theta'_{iter-1}, \quad (1)$$

where  $\theta'$  and  $\theta$  represent the parameters of the teacher and student models.  $\lambda$  is the smoothing coefficient, and  $iter$  indicates the training iteration step.

## 4 Experiments

### 4.1 Datasets

We use the following datasets for experiments. **ActivityNet v1.3 (ANET)** [5] consists of 20,000 videos that cover 200 action categories. Since its target categories are about activity or event, only 1 – 2 of long action instances exist in a video. **THUMOS14 (TH14)** [13] contains 413 videos with 20 sports-related action categories. Here, about 15 action instances exist per video on average. **FineAction(FinAct)** [23] includes 16,732 videos, encompassing 106 different action classes. On average, each video in this dataset contains 6 action instances.

In contrast to THUMOS14, FineAction covers various domains, including not only sports but also actions related to household, socializing, and personal care activities. Therefore, FineAction would better evaluate the generalization capability of an action localizer.

For self-training data, we use the video ID provided in **Kinetics-600** [6] and scrape the full video from YouTube. After filtering out very long videos exceeding 2.5 hours, about 332k videos are collected. Then, we build its subsets of 5k, 10k, 50k, 100k, and 200k videos, where a larger set encompasses a smaller set.

## 4.2 Evaluation Metrics

We use the standard mean average precision (mAP) which is widely used to evaluate TAL methods. For **ZS-TAL benchmarks**, we follow the conventions [15, 28] that report the mAPs at different temporal intersection over union (tIoU) thresholds and their average:  $[0.3 : 0.1 : 0.7]$  and  $[0.5 : 0.05 : 0.95]$  tIoU values for THUMOS14 [13] and ActivityNet v1.3 [5]. For **OV-TAL benchmarks**, we report the mAP of all, base, and novel categories defined in each dataset at a tIoU of 0.5. These metrics are denoted by  $\text{mAP}_A^{50}$ ,  $\text{mAP}_B^{50}$ , and  $\text{mAP}_N^{50}$ , respectively.

Across the experiments, we report the mAPs of the framework trained in full-shot (**FS**), without self-training (**w/o ST**), and with self-training (ST) settings. With self-training, we present the results of using in-domain and open-domain data, denoted by (**ID-ST**) and (**OD-ST**), respectively.

## 4.3 Implementation Details

For the video VLM, we adopt ViFi-CLIP [34] which is based on ViT-Base/16 [11] visual encoder and is pre-trained as video-text pairs using the K400 dataset [7]. In the pre-processing step of inputs, we interpolate videos into 30 fps and resize frames to 256 pixels on the shorter side, followed by a center crop of 224. Regarding video feature extraction, we use the window size of 16 frames and stride size of 4 frames. For the textual prompt input, we directly use the action category name without any prompt engineering. We attach more configurations for training and inference, such as training epoch, learning rate, and NMS, in the supplementary material.

## 4.4 Main Results

We perform extensive experiments on the FineAction dataset from the OV-TAL benchmark to evaluate the effectiveness of our proposed method.

**Scalability Evaluation.** Tab. 1 shows that self-training using open-domain data achieves increasing  $\text{mAP}_B^{50}$  and  $\text{mAP}_N^{50}$  with larger volume and outperforms the results of using in-domain data. We achieve these noteworthy results without a specially designed loss function or pseudo-labeling strategy. This demonstrates the high potential of self-training for OV-TAL with large-scale web videos.

**Table 1: Scalability with varying volume of videos for self-training.**

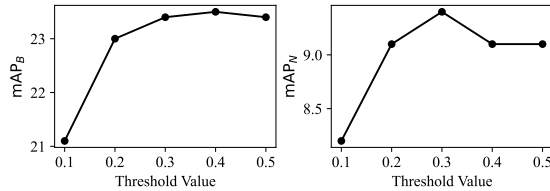
Extra Videos (#)	Generalized			Constrained	
	mAP <sub>A</sub> <sup>50</sup>	mAP <sub>B</sub> <sup>50</sup>	mAP <sub>N</sub> <sup>50</sup>	mAP <sub>B</sub> <sup>50</sup>	mAP <sub>N</sub> <sup>50</sup>
0k (w/o ST)	15.0	22.6	6.4	23.3	7.3
1.5k (ID-ST)	15.7	22.8	7.8	23.4	9.4
5k (OD-ST)	15.6	22.3	8.0	23.1	9.7
10k (OD-ST)	15.6	23.0	7.4	23.7	8.8
50k (OD-ST)	16.3	23.8	7.8	24.6	9.2
100k (OD-ST)	16.8	24.4	8.2	25.2	9.4
200k (OD-ST)	17.0	24.6	<b>8.5</b>	25.4	<b>9.9</b>
332k (OD-ST)	<b>17.2</b>	<b>25.1</b>	8.4	<b>25.8</b>	9.5
Full-Shot (FS)	18.8	23.5	13.5	24.5	16.0

**Table 2: Ablation study of VLMs as backbone.**

VLM	Generalized			Constrained	
	mAP <sub>A</sub> <sup>50</sup>	mAP <sub>B</sub> <sup>50</sup>	mAP <sub>N</sub> <sup>50</sup>	mAP <sub>B</sub> <sup>50</sup>	mAP <sub>N</sub> <sup>50</sup>
CLIP-B [33]	10.3	15.2	4.8	16.0	5.7
ViCLIP-B [39]	11.6	16.2	<b>6.5</b>	17.6	7.6
ViCLIP-L [39]	12.9	18.7	<b>6.5</b>	19.9	<b>7.9</b>
ViFi-CLIP-B [34]	<b>15.0</b>	<b>22.6</b>	6.4	<b>23.3</b>	7.3

**Table 3: Ablation study of score fusion methods.**

Score Fusion	Generalized			Constrained	
	mAP <sub>A</sub> <sup>50</sup>	mAP <sub>B</sub> <sup>50</sup>	mAP <sub>N</sub> <sup>50</sup>	mAP <sub>B</sub> <sup>50</sup>	mAP <sub>N</sub> <sup>50</sup>
Geometric Mean	<b>15.0</b>	<b>22.6</b>	<b>6.4</b>	<b>23.3</b>	<b>7.3</b>
Arithmetic Mean	13.5	20.5	5.6	21.4	6.7
Actionness Score ( $s_a$ )	13.9	21.7	5.2	22.4	6.0
Category Score ( $s_c$ )	1.0	1.4	0.5	1.3	0.5

**Fig. 5: Sensitivity analysis of pseudo-labels in self-training.**

The categories of scraped videos most likely belong to  $\mathcal{C}_B$  since Kinetics dataset [7] is used for sourcing videos for self-training and deciding  $\mathcal{C}_B$ . Thus, the improvement in mAP<sub>B</sub> is consistent, compared to fluctuating mAP<sub>N</sub>.

**VLM Backbone.** Tab. 2 presents the results of using different VLMs for STOV-TAL. Both ViCLIP and ViFi-CLIP outperform CLIP, benefiting from fine-tuning on large-scale video-text data. ViCLIP shows higher mAP<sub>N</sub>, while ViFi-CLIP exhibits mAP<sub>B</sub> since it is trained on Kinetics data, whereas ViCLIP is trained on newly crawled YouTube videos.

**Score Fusion.** Tab. 3 studies the score fusion method used in the inference time. The mAP significantly decreases without relying on the actionness score since the background category is not modeled in our frozen VLM. The arithmetic mean operation shows the lower mAPs than only using the  $s_a$  since some high  $s_c$  may dominate the final score. The different scale between  $s_a$  and  $s_c$  is caused by the different normalization operations, *e.g.*, sigmoid and softmax functions. On the other hand, the geometric mean operation alleviates this problem and leads to optimal performance.

**Robustness of Self-training.** One of the important factors in self-training is whether it is robust against the threshold values used for pseudo-labels. As

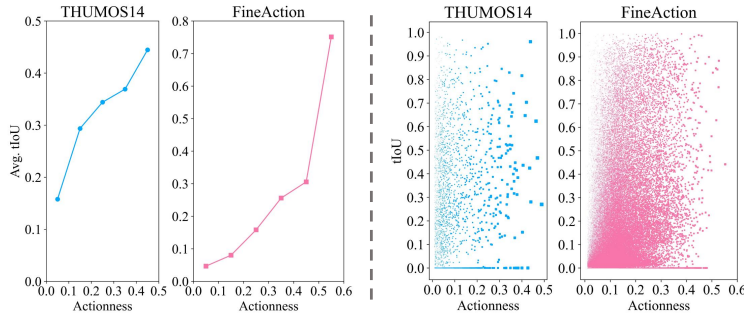


**Fig. 6: Quality analysis of pseudo-labels.** Correlation between the actionness of pseudo-labels and their tIoU between GT instances is measured on THUMOS14 and FineAction. The left graphs show the average of tIoU values in each interval of actionness (0.1). The right graphs show the scatter plot.

**Table 4: Evaluation of cross-category OV-TAL benchmark.** For (w/o ST), the model is trained on  $\mathcal{C}_B$  of target benchmark (TH14/FinAct). For (ID-ST), training videos of  $\mathcal{C}_N$  of the target benchmark are used. For (OD-ST), web-scraped videos are utilized. For reference of upper-bound, full-shot results are shown in gray. <sup>†</sup> indicates our reproduced results.

Methods	Backbone	THUMOS14					FineAction				
		Generalized			Constrained		Generalized			Constrained	
		mAP <sub>A</sub> <sup>50</sup>	mAP <sub>B</sub> <sup>50</sup>	mAP <sub>N</sub> <sup>50</sup>	mAP <sub>B</sub> <sup>50</sup>	mAP <sub>N</sub> <sup>50</sup>	mAP <sub>A</sub> <sup>50</sup>	mAP <sub>B</sub> <sup>50</sup>	mAP <sub>N</sub> <sup>50</sup>	mAP <sub>B</sub> <sup>50</sup>	mAP <sub>N</sub> <sup>50</sup>
OpenTAL <sup>†</sup> [1]	I3D [7]	30.2	42.7	11.3	42.6	11.9	6.2	10.4	1.4	11.0	1.8
STOV-TAL (w/o ST)	ViFi-CLIP-B [34]	45.7	<b>66.0</b>	15.3	<b>65.9</b>	16.2	15.0	22.6	6.4	23.3	7.3
STOV-TAL (ID-ST)	ViFi-CLIP-B [34]	<b>46.6</b>	65.8	<b>17.9</b>	65.8	<b>18.2</b>	15.7	22.8	7.8	23.4	9.4
STOV-TAL (OD-ST)	ViFi-CLIP-B [34]	44.2	62.6	16.7	62.5	17.0	<b>17.2</b>	<b>25.1</b>	<b>8.4</b>	<b>25.8</b>	<b>9.5</b>
STOV-TAL (FS)	ViFi-CLIP-B [34]	50.2	65.8	26.8	66.0	27.5	18.8	23.5	13.5	24.5	16.0

shown in Fig. 5, the self-training method can achieve consistent performance when we filter out the noisy action instances with a low confidence score.

**Quality of Pseudo-labels.** Fig. 6 shows the evident positive correlation between the actionness score and tIoU with GT action instances in the pseudo-labels. On the right side, we can observe that low-confident predictions are densely located at low tIoU values. Thus, filtering out pseudo-labels with very low actionness scores is sufficient to achieve decent performance.

#### 4.5 Results of OV-TAL Benchmark

We present the comparison with the previous method using OpenTAL [1] with ViFi-CLIP for classification due to the absence of reproducible OV-TAL methods [15, 28]. The details of using OpenTAL for OV-TAL are attached in supp.

**Cross-category Evaluation.** Tab. 4 shows our results in generalized and constrained ZS evaluation. The mAPs of unseen classes ( $\mathcal{C}_N$ ) are lower than those in Tab. 6. This reflects the difficulty of detecting rare actions that less frequently occur in training data.

Self-training the model with in-domain data improves mAP<sub>N</sub><sup>50</sup> in both THUMOS14 and FineAction. Using open-domain data also enhances the gain of

**Table 5: Evaluation of cross-dataset OV-TAL benchmark.** For (w/o ST), the model is trained on  $\mathcal{C}_B$  of TH14. For (ID-ST), all training videos of FinAct, including  $\mathcal{C}_B$  and  $\mathcal{C}_N$ , are used as the source data for self-training. For (OD-ST), web-scraped videos are exploited. <sup>†</sup> indicates our reproduced results.

Methods	Backbone	THUMOS14					FineAction				
		Generalized			Constrained		Generalized			Constrained	
		mAP <sub>A</sub> <sup>50</sup>	mAP <sub>B</sub> <sup>50</sup>	mAP <sub>N</sub> <sup>50</sup>	mAP <sub>B</sub> <sup>50</sup>	mAP <sub>N</sub> <sup>50</sup>	mAP <sub>A</sub> <sup>50</sup>	mAP <sub>B</sub> <sup>50</sup>	mAP <sub>N</sub> <sup>50</sup>	mAP <sub>B</sub> <sup>50</sup>	mAP <sub>N</sub> <sup>50</sup>
OpenTAL <sup>†</sup> [1]	I3D [7]	30.2	42.7	11.3	42.6	11.9	3.7	5.7	1.4	5.1	1.7
STOV-TAL (w/o ST)	ViFi-CLIP-B [34]	<b>45.7</b>	<b>66.0</b>	15.3	<b>65.9</b>	16.2	6.3	9.5	2.7	9.7	3.6
STOV-TAL (ID-ST)	ViFi-CLIP-B [34]	44.2	64.4	13.9	64.5	14.5	<b>7.4</b>	<b>11.0</b>	<b>3.4</b>	<b>11.2</b>	<b>4.4</b>
STOV-TAL (OD-ST)	ViFi-CLIP-B [34]	44.2	62.6	<b>16.7</b>	62.5	<b>17.0</b>	6.9	10.1	3.2	10.3	4.0

mAP<sub>N</sub><sup>50</sup>, indicating that our self-training method significantly boosts the model’s cross-category generalization ability. Although self-training with open-domain data results in a lower mAP<sub>B</sub><sup>50</sup>, this is justified by cross-dataset evaluation.

**Cross-dataset Evaluation.** Tab. 5 presents the results of cross-dataset generalization. Under both ID-ST and OD-ST settings, we can observe the improvement of all categories in FineAction, compared to the results without self-training. This demonstrates the enhanced cross-dataset generalization ability from the self-training with web-scraped data.

However, dropped mAPs of TH14 under ID-ST indicate that the model is fitted to the target dataset. In contrast, with open-domain data, mAP<sub>N</sub> increases, supporting its potential of achieving generalization ability in diverse domains.

#### 4.6 Results of ZS-TAL Benchmark

Tab. 6 presents the results of existing methods and ours in the ZS-TAL benchmark. First, we validate the effectiveness of our decoupled architecture, STOV-TAL. In both full-shot and zero-shot evaluation, a large improvement is shown by replacing the VLM backbone from CLIP [33] to ViFi-CLIP [34]. Based on this result, we expect higher mAPs by adopting the advanced video-language models, supporting the expandability of our framework. While mAPs of STOV-TAL are lower than those of ActionFormer in full-shot evaluation, ActionFormer cannot perform zero-shot inference, and our VLM-based classifier is not fine-tuned on the TAL dataset.

In addition, the decoupled architecture benefits from adopting the state-of-the-art action localizer. This is supported by the results from the zero-shot evaluation, comparing STOV-TAL (w/o ST) and the others using the same VLM backbone (CLIP-B). Our VLM-based action classifier is not fine-tuned on the benchmark, compared to the others adopting the prompt-tuning paradigm [53] to fine-tune and improve action classification accuracy. Thus, our high mAP is attributed to the enhanced action localizer. Note that the others show higher mAP in the full-shot results, but these are due to the fine-tuned classifier.

In THUMOS14, significant improvements are achieved from self-training with in-domain data. For example, with a tIoU at 0.5, mAP increases as 31.4  $\rightarrow$  34.4 and 34.3  $\rightarrow$  37.5 on 50%–50% and 75%–25% zero-shot evaluation, respectively.

**Table 6: Evaluation of ZS-TAL benchmark.** The results are based on RGB only without optical flow. In each setting, the best for each metric is bolded. Full-shot results are shown in gray for reference of upper-bound. † indicates our reproduced results. The values not provided are filled by “-”.

Evaluation Setting	Methods	Backbone	THUMOS14 [13]					ActivityNet v1.3 [5]				
			0.3	0.4	0.5	0.6	0.7	Avg.	0.5	0.75	0.95	Avg.
Full-shot 100% Seen 0% Unseen	ActionFormer† [48]	ViFi-CLIP-B [34]	72.8	67.4	57.3	45.2	29.7	54.5	49.5	31.2	4.3	30.9
	EffPrompt [15]	CLIP-B [33]	50.8	44.1	35.8	25.7	15.7	34.5	44.0	27.0	5.1	27.3
	STALE [28]	CLIP-B [33]	60.6	53.2	44.6	36.8	26.7	44.4	54.3	34.0	7.7	34.3
	UnLoc [46]	CLIP-B [33]	-	-	-	-	-	-	54.6	-	-	-
	UnLoc [46]	CLIP-L [33]	-	-	-	-	-	-	59.3	-	-	-
	STOV-TAL (FS)	CLIP-B [33]	47.5	41.7	33.0	24.7	15.4	32.5	37.5	23.1	1.8	22.7
	STOV-TAL (FS)	ViFi-CLIP-B [34]	65.3	60.6	50.2	39.0	26.0	48.2	43.7	26.8	2.0	26.4
Zero-shot 75% Seen 25% Unseen	EffPrompt [15]	CLIP-B [33]	39.7	31.6	23.0	14.9	7.5	23.3	37.6	22.9	3.8	23.1
	STALE [28]	CLIP-B [33]	40.5	32.3	23.5	15.3	7.6	23.8	38.2	25.2	<b>6.0</b>	24.9
	UnLoc [46]	CLIP-B [33]	-	-	-	-	-	-	40.2	-	-	-
	UnLoc [46]	CLIP-L [33]	-	-	-	-	-	-	48.8	-	-	-
	Ju <i>et al.</i> [16]	CLIP-B [33]	46.3	39.0	29.5	18.3	8.7	28.4	42.0	25.8	3.2	25.9
	STOV-TAL (w/o ST)	CLIP-B [33]	47.8	39.1	28.4	17.6	9.1	28.4	47.0	28.1	1.6	27.9
	STOV-TAL (w/o ST)	ViFi-CLIP-B [34]	56.7	47.2	34.3	22.8	11.3	34.5	51.7	<b>30.9</b>	1.8	<b>30.5</b>
	STOV-TAL (ID-ST)	ViFi-CLIP-B [34]	<b>59.5</b>	<b>50.2</b>	<b>37.5</b>	<b>24.6</b>	<b>12.5</b>	<b>36.9</b>	<b>52.0</b>	30.6	1.2	30.1
	STOV-TAL (OD-ST)	ViFi-CLIP-B [34]	58.2	48.2	35.1	23.0	11.8	35.2	-	-	-	-
	STOV-TAL (FS)	ViFi-CLIP-B [34]	67.5	60.8	47.7	34.8	21.8	46.5	52.6	31.5	2.3	31.3
Zero-shot 50% Seen 50% Unseen	EffPrompt [15]	CLIP-B [33]	37.2	29.6	21.6	14.0	7.2	21.9	32.0	19.3	2.9	19.6
	STALE [28]	CLIP-B [33]	38.3	30.7	21.2	13.8	7.0	22.2	32.1	20.7	<b>5.9</b>	20.5
	UnLoc [46]	CLIP-B [33]	-	-	-	-	-	-	36.9	-	-	-
	UnLoc [46]	CLIP-L [33]	-	-	-	-	-	-	43.7	-	-	-
	Ju <i>et al.</i> [16]	CLIP-B [33]	42.3	34.7	25.8	16.2	7.5	25.3	34.3	20.8	3.0	21.0
	STOV-TAL (w/o ST)	CLIP-B [33]	44.2	35.7	25.7	16.5	8.0	26.0	42.1	25.0	1.3	24.8
	STOV-TAL (w/o ST)	ViFi-CLIP-B [34]	53.4	43.1	31.1	19.7	9.8	31.5	48.1	28.4	1.3	<b>28.0</b>
	STOV-TAL (ID-ST)	ViFi-CLIP-B [34]	<b>56.3</b>	<b>46.1</b>	<b>34.4</b>	<b>21.9</b>	<b>11.3</b>	<b>34.0</b>	<b>48.4</b>	<b>28.7</b>	0.8	27.9
	STOV-TAL (OD-ST)	ViFi-CLIP-B [34]	54.3	43.7	32.5	21.4	10.6	32.5	-	-	-	-
	STOV-TAL (FS)	ViFi-CLIP-B [34]	68.2	62.5	50.7	38.2	24.6	48.8	49.4	29.9	2.2	29.6

In THUMOS14, using open-domain data results in smaller improvements as the evaluation split of the dataset is confined to the relatively narrow sports domain.

Self-training shows only marginal improvement on the ActivityNet dataset. This is attributed to the characteristics of ActivityNet which lacks the diversity of action duration. In zero-shot evaluation, the mAP of ZS nearly matches that of FS under the same VLM; for instance, in the 75%–25% split, the mAP of ZS and FS, with a tIoU at 0.5, are 51.7 and 52.6, respectively, showing a gap of only 0.9. This suggests that ActivityNet does not demand cross-category generalization in action localization, resulting in limited gains from self-training.

## 5 Conclusion

In this study, we investigated the scalability of action localization in the OV-TAL setting. Through the utilization of large-scale web data, we demonstrated significant improvements in the generalizability of class-agnostic action localizers. Coupled with a rigorous evaluation protocol we proposed, we aim for our work to serve as a robust benchmark for future research in this field.

## References

1. Bao, W., Yu, Q., Kong, Y.: Opental: Towards open set temporal action localization. In: CVPR. pp. 2979–2989 (2022) [1](#), [4](#), [12](#), [13](#), [19](#), [20](#)
2. Bird, S., Klein, E., Loper, E.: Natural language processing with Python: analyzing text with the natural language toolkit. " O'Reilly Media, Inc." (2009) [6](#)
3. Bodla, N., Singh, B., Chellappa, R., Davis, L.S.: Soft-nms—improving object detection with one line of code. In: ICCV. pp. 5561–5569 (2017) [8](#), [9](#)
4. Brown, T., Mann, B., Ryder, N., Subbiah, M., Kaplan, J.D., Dhariwal, P., Neelakantan, A., Shyam, P., Sastry, G., Askell, A., et al.: Language models are few-shot learners. NeurIPS **33**, 1877–1901 (2020) [4](#)
5. Caba Heilbron, F., Escorcia, V., Ghanem, B., Carlos Niebles, J.: Activitynet: A large-scale video benchmark for human activity understanding. In: CVPR. pp. 961–970 (2015) [9](#), [10](#), [14](#), [18](#), [19](#)
6. Carreira, J., Noland, E., Banki-Horvath, A., Hillier, C., Zisserman, A.: A short note about kinetics-600. arXiv preprint arXiv:1808.01340 (2018) [9](#), [10](#)
7. Carreira, J., Zisserman, A.: Quo vadis, action recognition? a new model and the kinetics dataset. In: CVPR. pp. 6299–6308 (2017) [3](#), [4](#), [6](#), [10](#), [11](#), [12](#), [13](#), [19](#), [20](#)
8. Cherti, M., Beaumont, R., Wightman, R., Wortsman, M., Ilharco, G., Gordon, C., Schuhmann, C., Schmidt, L., Jitsev, J.: Reproducible scaling laws for contrastive language-image learning. In: CVPR. pp. 2818–2829 (2023) [4](#)
9. Deng, J., Dong, W., Socher, R., Li, L.J., Li, K., Fei-Fei, L.: Imagenet: A large-scale hierarchical image database. In: CVPR. pp. 248–255. IEEE (2009) [4](#)
10. Devlin, J., Chang, M.W., Lee, K., Toutanova, K.: Bert: Pre-training of deep bidirectional transformers for language understanding. In: NACCL. pp. 4171–4186 (2019) [1](#)
11. Dosovitskiy, A., Beyer, L., Kolesnikov, A., Weissenborn, D., Zhai, X., Unterthiner, T., Dehghani, M., Minderer, M., Heigold, G., Gelly, S., Uszkoreit, J., Houshy, N.: An image is worth 16x16 words: Transformers for image recognition at scale. In: ICLR (2021), <https://openreview.net/forum?id=YicbFdNTTy> [10](#)
12. He, K., Gkioxari, G., Dollár, P., Girshick, R.: Mask r-cnn. In: ICCV. pp. 2961–2969 (2017) [8](#)
13. Idrees, H., Zamir, A.R., Jiang, Y.G., Gorban, A., Laptev, I., Sukthankar, R., Shah, M.: The thumos challenge on action recognition for videos “in the wild”. CVIU **155**, 1–23 (2017) [3](#), [9](#), [10](#), [14](#), [18](#), [19](#)
14. Jia, C., Yang, Y., Xia, Y., Chen, Y.T., Parekh, Z., Pham, H., Le, Q., Sung, Y.H., Li, Z., Duerig, T.: Scaling up visual and vision-language representation learning with noisy text supervision. In: ICML. pp. 4904–4916. PMLR (2021) [4](#)
15. Ju, C., Han, T., Zheng, K., Zhang, Y., Xie, W.: Prompting visual-language models for efficient video understanding. In: ECCV. pp. 105–124. Springer (2022) [2](#), [3](#), [4](#), [5](#), [6](#), [8](#), [10](#), [12](#), [14](#), [18](#), [19](#)
16. Ju, C., Li, Z., Zhao, P., Zhang, Y., Zhang, X., Tian, Q., Wang, Y., Xie, W.: Multi-modal prompting for low-shot temporal action localization. arXiv preprint arXiv:2303.11732 (2023) [4](#), [14](#)
17. Li, H., Wu, Z., Shrivastava, A., Davis, L.S.: Rethinking pseudo labels for semi-supervised object detection. In: AAAI. vol. 36, pp. 1314–1322 (2022) [8](#)
18. Li, J., Li, D., Xiong, C., Hoi, S.: Blip: Bootstrapping language-image pre-training for unified vision-language understanding and generation. In: ICML. pp. 12888–12900. PMLR (2022) [4](#)

19. Lin, C., Xu, C., Luo, D., Wang, Y., Tai, Y., Wang, C., Li, J., Huang, F., Fu, Y.: Learning salient boundary feature for anchor-free temporal action localization. In: CVPR. pp. 3320–3329 (2021) [7](#), [18](#)
20. Lin, T., Liu, X., Li, X., Ding, E., Wen, S.: Bmn: Boundary-matching network for temporal action proposal generation. In: ICCV. pp. 3889–3898 (2019) [2](#), [7](#), [8](#), [18](#)
21. Lin, T.Y., Goyal, P., Girshick, R., He, K., Dollár, P.: Focal loss for dense object detection. In: ICCV. pp. 2980–2988 (2017) [8](#)
22. Lin, W., Karlinsky, L., Shvetsova, N., Possegger, H., Kozinski, M., Panda, R., Feris, R., Kuehne, H., Bischof, H.: Match, expand and improve: Unsupervised finetuning for zero-shot action recognition with language knowledge. In: ICCV. pp. 2851–2862 (2023) [4](#)
23. Liu, Y., Wang, L., Wang, Y., Ma, X., Qiao, Y.: Fineaction: A fine-grained video dataset for temporal action localization. IEEE TIP **31**, 6937–6950 (2022) [2](#), [9](#), [18](#), [19](#)
24. Long, F., Yao, T., Qiu, Z., Tian, X., Luo, J., Mei, T.: Learning to localize actions from moments. In: ECCV. pp. 137–154. Springer (2020) [4](#)
25. Loshchilov, I., Hutter, F.: Decoupled weight decay regularization. In: ICLR (2019) [19](#)
26. Ma, C., Liu, Y., Deng, J., Xie, L., Dong, W., Xu, C.: Understanding and mitigating overfitting in prompt tuning for vision-language models. IEEE TCSVT (2023) [3](#)
27. Mikolov, T., Sutskever, I., Chen, K., Corrado, G.S., Dean, J.: Distributed representations of words and phrases and their compositionality. NeurIPS **26** (2013) [1](#), [4](#)
28. Nag, S., Zhu, X., Song, Y.Z., Xiang, T.: Zero-shot temporal action detection via vision-language prompting. In: ECCV. pp. 681–697. Springer (2022) [2](#), [4](#), [10](#), [12](#), [14](#), [18](#), [19](#)
29. Nag, S., Goldstein, O., Roy-Chowdhury, A.K.: Semantics guided contrastive learning of transformers for zero-shot temporal activity detection. In: WACV. pp. 6243–6253 (2023) [1](#)
30. Ni, B., Peng, H., Chen, M., Zhang, S., Meng, G., Fu, J., Xiang, S., Ling, H.: Expanding language-image pretrained models for general video recognition. In: ECCV. Springer (2022) [4](#)
31. Pham, H., Dai, Z., Ghiasi, G., Kawaguchi, K., Liu, H., Yu, A.W., Yu, J., Chen, Y.T., Luong, M.T., Wu, Y., Tan, M., Le, Q.V.: Combined scaling for zero-shot transfer learning. Neurocomputing **555**, 126658 (2023) [4](#)
32. Phan, T., Vo, K., Le, D., Doretto, G., Adjeroh, D., Le, N.: Zeetad: Adapting pre-trained vision-language model for zero-shot end-to-end temporal action detection. In: WACV. pp. 7046–7055 (2024) [2](#), [19](#)
33. Radford, A., Kim, J.W., Hallacy, C., Ramesh, A., Goh, G., Agarwal, S., Sastry, G., Askell, A., Mishkin, P., Clark, J., et al.: Learning transferable visual models from natural language supervision. In: ICML. vol. 139, pp. 8748–8763. PMLR (2021) [2](#), [3](#), [4](#), [8](#), [11](#), [13](#), [14](#)
34. Rasheed, H., Khattak, M.U., Maaz, M., Khan, S., Khan, F.S.: Fine-tuned clip models are efficient video learners. In: CVPR. pp. 6545–6554 (2023) [3](#), [4](#), [5](#), [6](#), [10](#), [11](#), [12](#), [13](#), [14](#), [18](#), [19](#), [20](#)
35. Rathod, V., Seybold, B., Vijayanarasimhan, S., Myers, A., Gu, X., Birodkar, V., Ross, D.A.: Open-vocabulary temporal action detection with off-the-shelf image-text features. arXiv preprint arXiv:2212.10596 (2022) [4](#)
36. Sennrich, R., Haddow, B., Birch, A.: Neural machine translation of rare words with subword units. In: ACL. vol. 1, pp. 1715–1725 (2016) [8](#)

37. Tarvainen, A., Valpola, H.: Mean teachers are better role models: Weight-averaged consistency targets improve semi-supervised deep learning results. *NeurIPS* **30** (2017) [9](#)
38. Wang, L., Xiong, Y., Lin, D., Van Gool, L.: Untrimmednets for weakly supervised action recognition and detection. In: *CVPR*. pp. 4325–4334 (2017) [19](#)
39. Wang, Y., He, Y., Li, Y., Li, K., Yu, J., Ma, X., Chen, X., Wang, Y., Luo, P., Liu, Z., et al.: Internvid: A large-scale video-text dataset for multimodal understanding and generation. *arXiv preprint arXiv:2307.06942* (2023) [4](#), [11](#), [18](#)
40. Wang, Y., Chen, H., Heng, Q., Hou, W., Fan, Y., Wu, Z., Wang, J., Savvides, M., Shinozaki, T., Raj, B., Schiele, B., Xie, X.: Freematch: Self-adaptive thresholding for semi-supervised learning. In: *ICLR* (2023) [9](#)
41. Weng, Z., Yang, X., Li, A., Wu, Z., Jiang, Y.G.: Open-VCLIP: Transforming CLIP to an open-vocabulary video model via interpolated weight optimization. In: *ICML*. vol. 202, pp. 36978–36989. PMLR (2023) [4](#)
42. Wu, J., Li, X., Xu, S., Yuan, H., Ding, H., Yang, Y., Li, X., Zhang, J., Tong, Y., Jiang, X., et al.: Towards open vocabulary learning: A survey. *IEEE TPAMI* (2024) [1](#)
43. Xia, K., Wang, L., Zhou, S., Hua, G., Tang, W.: Learning from noisy pseudo labels for semi-supervised temporal action localization. In: *ICCV*. pp. 10160–10169 (October 2023) [8](#)
44. Xian, Y., Lampert, C.H., Schiele, B., Akata, Z.: Zero-shot learning—a comprehensive evaluation of the good, the bad and the ugly. *IEEE TPAMI* **41**(9), 2251–2265 (2018) [6](#)
45. Xu, M., Zhao, C., Rojas, D.S., Thabet, A., Ghanem, B.: G-tad: Sub-graph localization for temporal action detection. In: *CVPR*. pp. 10156–10165 (2020) [7](#), [18](#)
46. Yan, S., Xiong, X., Nagrani, A., Arnab, A., Wang, Z., Ge, W., Ross, D., Schmid, C.: Unloc: A unified framework for video localization tasks. In: *ICCV*. pp. 13623–13633 (2023) [4](#), [14](#)
47. Zareian, A., Rosa, K.D., Hu, D.H., Chang, S.F.: Open-vocabulary object detection using captions. In: *CVPR*. pp. 14393–14402 (2021) [2](#)
48. Zhang, C.L., Wu, J., Li, Y.: Actionformer: Localizing moments of actions with transformers. In: *ECCV*. pp. 492–510. Springer (2022) [6](#), [7](#), [14](#), [18](#)
49. Zhang, L., Chang, X., Liu, J., Luo, M., Wang, S., Ge, Z., Hauptmann, A.: Zstad: Zero-shot temporal activity detection. In: *CVPR*. pp. 879–888 (2020) [1](#), [4](#), [6](#)
50. Zhang, Y., Zhang, X.Y., Shi, H.: Ow-tal: learning unknown human activities for open-world temporal action localization. *Pattern Recognition* **133**, 109027 (2023) [1](#)
51. Zheng, Z., Wang, P., Liu, W., Li, J., Ye, R., Ren, D.: Distance-iou loss: Faster and better learning for bounding box regression. In: *AAAI*. vol. 34, pp. 12993–13000 (2020) [8](#)
52. Zhou, K., Yang, J., Loy, C.C., Liu, Z.: Conditional prompt learning for vision-language models. In: *CVPR*. pp. 16816–16825 (2022) [3](#)
53. Zhou, K., Yang, J., Loy, C.C., Liu, Z.: Learning to prompt for vision-language models. *IJCV* **130**(9), 2337–2348 (2022) [13](#)

## Appendix

In this section, we provide additional experimental results and details not presented in the main paper.

### A Additional Implementation Details

We primarily adopt the hyperparameters from ActionFormer [48] and ViFi-CLIP [34] since our architecture is based on them. As addressed in Sec. 4.1, the ActivityNet [5] dataset differs significantly from the THUMOS14 [13] and FineAction [23] datasets. It consists of only 1 – 2 long action instances, limiting the evaluation of the capability in action localization. Accordingly, we adjust hyperparameters for the ActivityNet dataset, following the TAL literature.

#### A.1 Video Feature Extraction Details

Here, we detail the video feature extraction process using VLMs. As stated in Sec. 4.3, we extract the video snippet features ( $\mathbf{F}_v$ ) using the conventional sliding window manner with a window size of 16 frames and a stride size of 4 frames, after interpolating videos into 30 fps. For ActivityNet, we interpolate  $\mathbf{F}_v$  to a fixed length following the widely used convention [19, 20, 45, 48]. Specifically, each video is interpolated to a length of 192 feature vectors, as employed in ActionFormer [48]. For THUMOS14 and FineAction, we retain the video snippet features in their original length. For the experiments with ViCLIP [39], we interpolate its learned temporal embedding from 8 to 16 to use the same window size for video feature extraction. Note that such details are often absent in existing OV-TAL methods [15, 28], making it challenging to reproduce their results. We will release the extracted features to encourage the OV-TAL community.

#### A.2 Inference Details

Compared to ActionFormer [48], we use the class-agnostic action localizer and assign the action classes from the VLM. As a result of this change, we delay the Soft-NMS operation until after the action classes are assigned, rather than immediately following the output of the action localizer. On the other hand, when we compute pseudo labels on unlabeled videos, we directly perform Soft-NMS on the class-agnostic action instances, based on its actionness score ( $s_a$ ). We employ the same Soft-NMS configurations for both cases, with slight variations based on the dataset. We choose the top 100 scoring action instances for ActivityNet and 200 for THUMOS14 and FineAction, applying a minimum confidence score threshold of 0.001 and a tIoU threshold of 0.1.

**Table 7: Training hyperparameters values.**

Dataset	Stage	max lr	warm-up epoch	main epoch	batch size
ActivityNet	First	$1e^{-5}$	5	10	16
	Second	$1e^{-5}$	5	5	16
THUMOS14	First	$1e^{-4}$	5	30	2
	Second (ID-ST)	$1e^{-4}$	5	10	2
FineAction	First	$1e^{-5}$	5	10	4
	Second (ID-ST)	$1e^{-5}$	5	5	4
THUMOS14 FineAction	Second (OD-ST)	$1e^{-5}$	2	2	4

### A.3 Selection of Previous Methods for OV-TAL

Including the results of existing OV-TAL methods [15, 28, 32] in our proposed OV-TAL benchmarks would be a good practice to ensure a sufficient comparison. However, due to the difficulty of reproducing their results<sup>1</sup>, we instead choose OpenTAL [1], which focuses on localizing actions unseen during training through uncertainty modeling. We train it on the base categories defined in our OV-TAL benchmark and use it as the class-agnostic action localizer in our decoupled architecture. Although OpenTAL utilizes the I3D [7] backbone for action localization, we assign action classes to output action instances using ViFi-CLIP [34], as same as our model. Thus, comparing its mAPs with ours solely evaluates the capability of action localization.

### A.4 Training Details

AdamW [25] is chosen as the optimizer, coupled with a scheduler that linearly warms up the learning rate (lr) to its maximum value and decays to the minimum value ( $1e^{-8}$ ) following a cosine function. Tab. 7 presents the hyperparameter values for each dataset. For the OD-ST experiments on THUMOS14, we use the subset of 100k videos. We empirically found the threshold values for obtaining pseudo labels. 0.2, 0.05, and 0.4 are used for ActivityNet, THUMOS14, and FineAction, respectively.

## B Additional Experimental Results

### B.1 ActivityNet v1.3 Results for OV-TAL Benchmark

The main paper presents the cross-category OV-TAL benchmark results of the THUMOS14 [13] and FineAction [23] datasets in Tab. 4. Here, we show the results of the ActivityNet v1.3 [5] in Tab. 8. As discussed in Sec. 4.6, ActivityNet v1.3 is not a proper dataset for evaluating the generalization capability in action localization, supported by the zero-shot performance (w/o ST) of action localization on par with that of full-shot in Tab. 6. In the proposed OV-TAL benchmark,

<sup>1</sup>In Issue 1 and Issue 2, the author mentioned that the method exploits UNet [38] as the external action classifier which is trained on all action classes in the dataset.

**Table 8: Evaluation of cross-category OV-TAL benchmark.** For reference of upper-bound, full-shot results are shown in gray. <sup>†</sup> indicates our reproduced results.

Methods	Backbone	ActivityNet v1.3				
		Generalized			Constrained	
		mAP <sub>A</sub> <sup>50</sup>	mAP <sub>B</sub> <sup>50</sup>	mAP <sub>N</sub> <sup>50</sup>	mAP <sub>B</sub> <sup>50</sup>	mAP <sub>N</sub> <sup>50</sup>
OpenTAL <sup>†</sup> [1]	I3D [7]	32.7	36.4	29.7	39.1	34.1
<b>STOV-TAL (w/o ST)</b>	ViFi-CLIP-B [34]	42.9	47.5	39.1	51.3	44.1
<b>STOV-TAL (ID-ST)</b>	ViFi-CLIP-B [34]	43.1	47.3	39.7	51.1	44.6
STOV-TAL (FS)	ViFi-CLIP-B [34]	43.7	47.9	40.3	52.0	45.3

we observe a similar trend. For instance, in the constrained setting, mAP<sub>N</sub><sup>50</sup> of w/o ST and FS are 44.1 and 45.3, respectively. Based on these results, we decided not to include the ActivityNet dataset in the OV-TAL benchmark since there is only a small potential for improvement in cross-category generalization ability.